PHYSICAL REVIEW B VOLUME 21, NUMBER 10 15 MAY 1980

Extended x-ray absorption fine structure analysis of interatomic distances, coordination numbers, and mean relative displacements in disordered alloys

B. Lengeler* and P. Eisenberger
Bell Laboratories, Murray Hill, New Jersey 07974
(Received 31 May 1979)

A procedure is described for determining interatomic distances r, coordination numbers N, and mean relative displacements σ from extended x-ray absorption fine structure (EXAFS) data on disordered metallic systems. This procedure includes the case when the spectrometer has finite energy resolution. It is shown how the absolute value of the EXAFS can be determined. A way has been developed to determine the inelastic loss factors of the photoelectrons from model compounds of known structure. The procedure has been checked on four metallic systems (Cu, α-*Al*Cu, θ' and θ AlCu). The accuracy of the analysis is 1% for the interatomic distances, 15% for the coordination numbers, and 20% for σ. The reliability of the data analysis, which depends strongly on the number of different atoms in a shell, on the magnitude of their mean relative displacement and on the difference in their backscattering power will be discussed at length.

I. INTRODUCTION

Measurements of the fine structure above the absorption edges of x rays in condensed matter (EXAFS) have been used to an increasing extent over the last years for the determination of the local atomic arrangements in ordered and disordered systems.[1–16] In most previous investigations emphasis has been on the determination of the interatomic distances which can be measured by this technique with an accuracy of 1%. In this paper we will concentrate especially on the information contained in the amplitude of the EXAFS which allows one to determine coordination numbers and mean relative displacements. In order to analyze EXAFS spectra it is necessary to know the energy dependence of the scattering phases in the absorbing and in the backscattering atoms and the energy dependence of the scattering amplitude of the backscatterers. Scattering phases for pairs of absorbers and backscatterers have been shown to be transferable from one compound to another.[7] In the meantime *ab initio* calculations of the amplitudes and phases have become available for a large number of elements.[17]

The most widely used procedure of data processing is to Fourier transform the background-subtracted and normalized EXAFS oscillations into real space in order to separate the contributions of the different coordination shells around the absorbing atoms.[1,5,6,8] For those peaks in the Fourier spectrum which contain only one atomic species at one atomic distance the analysis of the distances and of the temperature dependence of the Debye-Waller factor are straightforward.[4,5] When the contribution of two shells are not resolved in the Fourier spectrum a more sophisticated data processing is necessary. One possibility is to construct a model for the system under investigation, to calculate its EXAFS oscillations, and to vary the parameters in such a way that its Fourier transform fits the Fourier spectrum of the measured data.[14] Another technique is Fourier filtering.[5,6,8,11,13] Here specific peaks in the Fourier spectrum are transformed back into k space (photoelectron momentum) and the resulting curves are fitted with the known EXAFS formula. We have adopted this procedure, and it is one of the aims of this paper to show the possibilities of the data processing chosen here on four different metallurgical systems of known structure and different complexity. These systems are pure Cu, a dilute *Al*Cu alloy in the α phase, and two AlCu phases called θ' and θ. We have measured the fine structure above the K edge of Cu in these systems at the Stanford Synchrotron Radiation Laboratory (SSRL). We will discuss at length the significance of the fitting procedure, especially its dependence on the number of different atoms in one shell, on their atomic number and on the correlation between the Debye-Waller factors and the coordination numbers.

Many spectrometers used to measure EXAFS have a finite-energy resolution. This leads to a smearing of the measured EXAFS. We will discuss the size of this effect and its influence on the determination of the coordination number and the Debye-Waller factor. We also give a modified version of the EXAFS formula which takes this effect into account. This effect is most serious for spectra measured on x-ray tubes and in some spectrometers used at synchrotrons (like on the focused beam line at SSRL).

A problem of great importance in the determina-

tion of the coordination numbers and Debye-Waller factors arises from inelastic scattering processes which reduce the fraction of photoelectrons contributing to the EXAFS interference.[1,2,14,16] For the first neighbor shell these losses are of the order of 50%. In most cases, this reduction was taken care of by an exponential damping with a mean free path which, in general, was treated as energy independent. We have adopted another approach by assigning to each pair of absorber and backscatterer and to each shell individual loss factors which were determined by means of model compounds with known structure. A comparison will be given for the two descriptions of the electron losses. The paper is organized as follows. In Sec. II we give a version of the EXAFS formula which takes into account the finite energy resolution of the spectrometer, the inelastic photoelectron losses and the normalization of the EXAFS which differs somewhat from the procedure used by other investigators. Section III gives experimental details concerning sample preparation and data collection. In Secs. IV and V we describe the experimental results and the data analysis, and we discuss the accuracy of the data obtained.

II. EXAFS EXPRESSION FOR s LEVEL EXCITATION

For the excitation of an s level (K, L_1) the normalized oscillatory component of the absorption coefficient μ is given for polycrystalline, not too strongly disordered systems by[1,18,19]

$$\tilde{\chi}(k) = (\mu - \mu_0)/\mu_0 = \sum_j \frac{N_j}{kr_j^2} \exp(-2\sigma_j^2 k^2) F_j(k) D_j \times \sin[2kr_j + \phi_j(k)] \quad . \tag{1}$$

k is the photoelectron wave vector defined by

$$k = [2m(E - E_0)/\hbar^2]^{1/2} \quad , \tag{2}$$

where E is the photon energy and E_0 the energy threshold of the absorption edge. $F_j(k)$ is the backscattering amplitude from each of the N_j neighbors of type j and at a distance r_j away from the absorbing atom. σ_j^2 is the mean square of the relative displacement between the absorber and the backscatter j. $\phi_j(k)$ is the total scattering phase shift experience by the photoelectron

$$\phi_j(k) = \phi_a(k) + \phi_b^j(k) - \pi \quad . \tag{3}$$

ϕ_a is the phase shift due to the absorbing atom and ϕ_b^j is the phase of the backscattering amplitude from the neighbor j. We have used in our analysis the backscattering amplitudes and phase shifts for Cu and Al calculated by Teo and Lee.[17] The factor D_j takes into account the photoelectron losses due to inelastic scattering processes. For p-level excitation (L_{II}, L_{III}) Teo *et al.*[17] have given the corresponding expression to Eq. (1). Since the main aspects which are of interest here are the same for s- and p-level excitation, we will confine to Eq. (1). In order to analyze experimental EXAFS spectra by means of Eq. (1), we have first to extend this expression in the following way.

A. Finite-energy resolution of the spectrometer

Due to the angular divergence of the x-ray beam emerging from a synchrotron or from an x-ray tube, a finite bandwidth passes through the monochromator crystal. The resulting smearing of the measured fine structure can affect the determination of the coordination numbers and of the Debye-Waller factor and hence must be corrected. We will now consider the magnitude of this effect at the focused beam line and at the EXAFS I beam line at SSRL. It is easy to transfer the results to other beam lines. At the focused beam line at SSRL the mirror collects the entire vertical divergence of the synchrotron radiation. For the beam condition which existed during our study, there was a vertical angular divergence $\Delta\theta$ of 3×10^{-4} radians. For a Ge (111) crystal with a lattice spacing of 3.2664 Å, this leads at the Cu K edge (1.38Å^{-1}) to an energy spread of 12.5 eV. On the other hand on the EXAFS I line at SSRL the vertical divergence of the synchrotron beam is defined by a slit 1 mm at 20 m giving $\Delta\theta = 5 \times 10^{-5}$ and $\Delta E = 1.17$ eV for a Si (220) monochromator at the Cu K edge. This energy spread is small and has been neglected in the following. In order to determine the energy resolution function of the focused spectrometer at SSRL, we have measured the EXAFS spectra of pure Cu at the EXAFS I line and at the focused beam line. We then have assumed that the resolution function can be described by a Gaussian of form

$$g(E - E')\,dE' = (2\pi\tau^2)^{-1/2} \exp[-(E - E')^2/2\tau^2]\,dE' \tag{4}$$

or with Eq. (2)

$$h(k,k')\,dk' = (2\pi\tau^2)^{-1/2}(\hbar^2 k'/m) \times \exp[-\hbar^4 k^2 (k' - k)^2/2\tau^2 m^2]\,dk' \quad . \tag{5}$$

Since the Gaussian is peaked at $k = k'$ we have replaced $(k'^2 - k'2)^2$ in the exponent by $4k^2(k' - k)^2$. The Cu EXAFS spectra measured on EXAFS I (and assumed to contain no smearing from finite-energy resolution) has now been convoluted with the resolution function Eq. (5) and τ varied until agreement was obtained with the spectrum measured on the focused beam line. Excellent agreement between the two curves was obtained for $\tau = 5.3$ eV. This confirmed the Gaussian as an adequate description of the

resolution function. The full width at half maximum (FWHM) value of the resolution is $2(2\ln 2)^{1/2}\tau = 12.5$ eV in good agreement with the value deduced from the beam divergence. The resolution of the focused beam line for other K edges can be determined from this value by means of Bragg's law

$$2(2\ln 2)^{1/2}\tau = 3\times 10^{-4} E \cot\theta \ , \tag{6}$$

where $\Delta\theta = 3\times 10^{-4}$ was taken from the τ value determined for Cu.

Energy smearing can also be a problem on the beam-line EXAFS I at SSRL or on similar lines, especially at higher photon energy. Indeed, at the Ag K edge a beam with a divergence of 1 mm at 20 m passing through a Si (220) monochromator has a width of 10 eV.

In order to take the finite energy resolution of the focused beam-line spectrometer at SSRL into account, we have convoluted the theoretical expression Eq. (1) with the resolution function (5) rather than deconvoluting the experimental results

$$\chi(k) = \int_{-\infty}^{\infty} \tilde{\chi}(k')\, h(k,k')\, dk' \ . \tag{7}$$

The sin factor in Eq. (1) creates the strong variations of χ whereas the other factors are slowly varying functions of k. Therefore, we extract the prefactors from the integral in Eq. (7) and convolute only the sin. If we take into account that the main k dependence of the argument of the sin is from $2kr_j$ and from the linear term of $\phi_j(k)$ we end up with an integral that can be solved analytically. The result of the convolution is

$$\chi(k) = \sum_j \frac{N_j}{kr_j^2} \exp(-2\sigma_j^2 k^2) F_j(k) D_j \times \exp[-(2r_j+\alpha_j)^2 m^2\tau^2/2\hbar^4 k^2] \times \sin[2kr_j + \phi_j(k)] \ . \tag{8}$$

The finite-energy resolution shows up as an exponential damping factor. The damping is large at small k and small for large k. α_j is the mean slope of $\phi_j(k)$

$$\phi_j(k) \cong \alpha_j k + \text{const.} \tag{9}$$

Typical values in Al-Cu alloys are $r_j = 2.5$ Å and $\alpha_j = -1$ Å. For $\tau = 5.3$ eV the damping is 0.79 at $k = 4$ Å^{-1} and 0.96 at $k = 10$ Å^{-1}. This shows that the effect of the finite-energy resolution on the focused beam lined at SSRL is not negligible and has to be taken into account if distances, coordination numbers and Debye-Waller factors are to be extracted from EXAFS data.

B. Absolute value of χ

The fine structure in the ratio of the photon intensities I_0/I measured in a transmission experiment is superposed on a smooth background. This background is energy dependent due to an energy dependence of the photon flux and of the absorption in the sample and in the ionization chambers.[4,6,20] In general, these effects are not known very well and thus the background in $\ln(I_0/I)$ is of unknown size. One possibility is to extrapolate the background below the K edge into the range of the EXAFS and to remove in a second step the smooth background of the K-shell absorption.[4,20] Another possibility is to subtract from the measured spectra the whole smooth background in one step by means of a series of spline functions.[13] We have adopted this approach. But it must be taken into account that the resulting oscillations are not $(\mu-\mu_0)/\mu_0 = \chi$ but $(\mu-\mu_0)d$ where d is the thickness of the sample. Before we can compare this with Eq. (1) we first need $\mu_0 d$. We have chosen in our analysis the following concept to obtain $\mu_0 d$. According to Heitler[21] the k dependence of the absorption coefficient of a gas in the vicinity of the K edge ($E \gtrsim E_0$) is proportional to

$$\mu_0 d \sim (1+k^2a^2)^{-4}[1-\exp(-2\pi/ka)]^{-1} \times \exp[-(4/ka)\arctan ka] \ ,$$

$$a^{-2} = 2mE_0/\hbar^2 \ .$$

For k values up to 16 Å^{-1} this can be written to a good approximation by

$$\mu_0 d \sim 1 - \tfrac{8}{3}k^2a^2 \ .$$

We have used this expression to describe the k dependence of the background $\mu_0 d$. Its absolute value at $k=0$ was taken from the jump J in $\ln(I_0/I)$ at the K edge, so that

$$\mu_0 d = J(1-\tfrac{8}{3}k^2a^2) \ . \tag{10}$$

C. Photoelectron losses

The photoelectron losses D_j due to inelastic scattering processes have often been described by an exponential damping factor[1,4,13]

$$D_j = \exp[-2r_j/\lambda(k)] \ , \tag{11}$$

where $\lambda(k)$ is the mean free path of the photoelectron. This concept is unsatisfactory in so far as the theoretical and empirical backscattering amplitudes $F_j(k)$ already include inelastic effects occurring in the backscatterer. In addition, the inelastic losses inside the absorbing atom cannot be described by a mean free path. Therefore, an expression of the form

$$D_j = \tilde{D}_j(k)\exp[-2r_j/\lambda(k)] \tag{12}$$

would be more appropriate. Here $\tilde{D}_j(k)$ takes care of those losses which are independent of the distance. On the other hand, at the present time Eq. (12) is of no help because $\tilde{D}_j$ is unknown and there is no gen-

eral form for the k dependence of $\lambda(k)$. The x-ray photoelectron spectroscopy (XPS), ultraviolet photoelectron spectroscopy (UPS), and Auger data collected in Ref. 22 show the wide spread in the values of λ between 4 and 10 Å in the energy range between 50 and 1000 eV. Furthermore, it is not possible by measuring the electron losses in model compounds to untangle the k dependence of $\bar{D}$ and of λ. In order to take into account the possibility of r-independent contributions in D_j we have chosen the following approach. We have assigned to each shell and to each pair of absorber-backscatterer a k-independent loss factor D_j. The D_j are determined from model compounds of chemical constitution as near as possible to the unknown system. We have also used an expression Eq. (11) for the electron losses with λ independent of k. A comparison of the two approaches will be given below.

Combining Eqs. (1), (8), and (10), we obtain the final expression for $(\mu-\mu_0)d$

$$(\mu=\mu_0)\equiv\Delta\chi d$$
$$=J(1-\tfrac{8}{3}k^2a^2)\sum_j N_j(kr_j^2)^{-1}D_j\exp(-2\sigma_j^2k^2)F_j(k)\exp[-(2r_j+\alpha_j)^2m^2\tau^2/2\hbar^4k^2]\sin[2kr_j+\phi_j(k)] \quad . \quad (13)$$

It is this expression with which the background subtracted EXAFS spectra are compared in order to determine the distances r_j, the coordination numbers N_j, and the Debye-Waller factors σ_j.

III. EXPERIMENTAL

The copper used in this investigation was a 10-μm-thick foil of high-purity Cu. The alloys used were a dilute AlCu alloy with 0.5 at.% Cu in the α phase[23] and two Al-Cu phases called θ' and θ.[24,25] At room temperature α–AlCu and θ' are metastable and can only be produced by an appropriate heat treatment of a supersaturated solid solution (SSSS) of Cu in Al. The phase θ can be obtained as a precipitation from a SSSS or by alloying appropriate amounts of the constituents. We have used alloys with 0.5 and 2 at.% Cu and an intermetallic compound θ, $CuAl_{2.05}$. They were prepared under high vacuum from $6N$ aluminum and $5N$ copper partly by inductive heating in a cold crucible and partly by melting the components in a graphite crucible in an oven. Great care was taken to reach a thorough mixing of the two components in the melt. The composition of the alloys was determined from the weight of the constituents. Losses by evaporation during the melt were negligible. The intermetallic compound was ground in a mortar into fine powder and annealed for 12 h in high vacuum at 550 °C to remove the strain produced by the grinding. A Debye-Scherrer analysis of the powder showed all lines quoted by Havinga *et al.*[24] but no additional lines within the accuracy of the analysis, which was better than 5%. The dilute alloy lumps were rolled into ribbons of about 250-μm thickness. Several ribbons of 7 cm were attached to a frame made out of molybdenum wire (0.5-mm thickness) and annealed for 2 h at 540 °C in a quartz tube. The setup used was similar to the one described in Ref. 26. High-purity argon gas was flowing at a rate of 2 liters per minute through the quartz tube. A copper bell surrounding the samples ensured a homogeneous temperature of the samples in the oven and a high quenching rate. The quenching bath was distilled water at 0 °C. Due to the fast quenching the starting point of the decomposition sequence is the supersaturated solid solution with an atomic arrangement similar to that in thermal equilibrium at 540 °C. In addition, the quenched samples contained about 100 ppm of vacancies.[26] About a minute after the quench different heat treatments were given to the samples in order to obtain the different stable and metastable precipitates mentioned above (Table I).

The measurement of the EXAFS spectra was done in transmission on the focused beam line at the Stanford Synchrotron Radiation Laboratory. The Stanford Position-Electron Asymmetric Ring (SPEAR) was operated at 3.3 GeV and about 20 mA. The photon flux at the Cu K edge was about 10^8 photons/sec eV behind the monochromator. Two parallel germanium crystals (111) with lattice spacing 3.2664 Å were used to monochromatize the radiation. The influence of the vertical divergece of the beam on the EXAFS spectra is considered in Sec. II. The incoming and transmitted radiation was monitored by means of two ionization chambers both filled with N_2 at one atmosphere. The photon energies were swept in 2-eV steps over an energy range of up to 1000 eV.

TABLE I. Heat treatment given to the different AlCu alloys after homogenization for 2 h at 540 °C and quenching into water at 0 °C in order to obtain the phases α, θ', and θ.

Cu concentration (at.%)	Time	T (°C)	Atmosphere	Phase
0.5	6 weeks	25	air	α-AlCu
2	6 h	240	argon	θ'
2	44 h	400	argon	θ

The recorded photon fluxes were digitized in a PDP 11 computer which also controls the energy sweep. The data were recorded on floppy discs and on magnetic tape. A typical run containing about 200 data points took about 15 min. All measurements were done at 77 K in order to keep the thermal damping of the EXAFS signal small. A simple styrofoam container with a double-window system made out of Mylar was used as cryostat. The samples were mounted on aluminum frames which were partly immersed in liquid nitrogen and could be exchanged within less than a minute.

IV. EXPERIMENTAL RESULTS AND DATA EVALUATION

A. Results for pure Cu

Figure 1 shows the EXAFS spectrum for a foil of pure Cu of 10-μm thickness measured at 77 K on the focused beam line at SSRL. Choosing a starting value $E_0 = 9005$ eV, we have first converted the energy scale into the k scale according to Eq. (2). Then the data are multiplied by k^3 to compensate for the decrease of the EXAFS amplitude at high k due to the Debye-Waller factor, the backscattering amplitude $F_j(k)$, and the factor $1/k$ in Eq. (1). Finally, a smooth background is subtracted from the EXAFS in order to separate the nonoscillatory part in $\ln(I_0/I)$. This background is described by a set of cubic splines.[13] The result of this operation is shown in Fig. 2 (full line). The data set is 15 Å^{-1} long and the smooth background was composed of five splines of equal length. Choosing the number of splines too small means that the background is not separated well enough but choosing its number too large means that the background follows the EXAFS oscillations. When the data set is multiplied by k^3 it turned out that the optimum number of splines is one for every 3–4 Å^{-1} of data in k space.

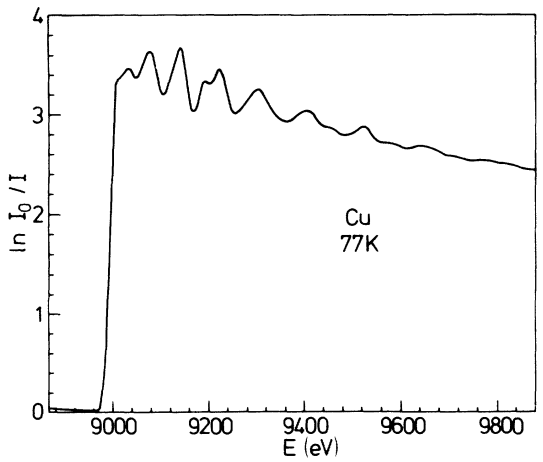

FIG. 1. EXAFS data for pure Cu at 77 K measured in transmission at the focused beam line at SSRL.

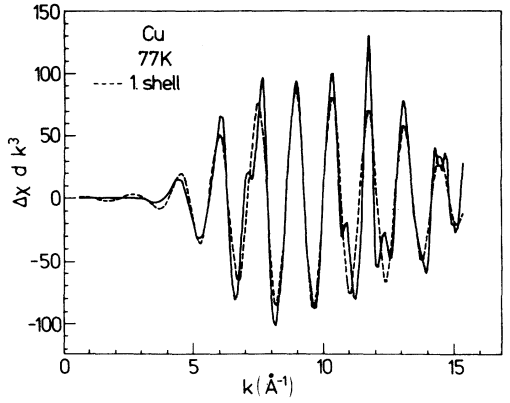

FIG. 2. EXAFS spectrum for pure Cu from Fig. 1 after background subtraction and multiplication by k^3 (full line). The contribution of the first shell is shown as dashed line.

In order to separate the contributions from the different shells we have Fourier transformed the EXAFS spectra $\Delta\chi dk^3$ by means of a fast-Fourier-transform routine. Figure 3 shows the absolute value of the Fourier spectrum. Five different shells are visible whereas the higher shells disappear in the noise. By means of a filter function (shown as a broken line in Fig. 3) the contribution of the first shell is separated from the rest of the spectrum.[13] The product of the spectrum with this filter function is Fourier backtransformed into k space and shown as a broken line in Fig. 2. The width of the filter function has been chosen in such a way that the peak under consideration is not altered by multiplication with the

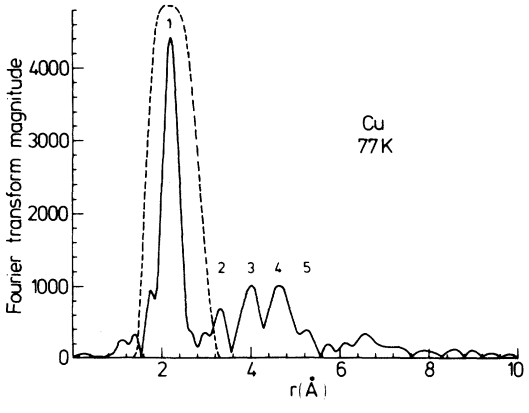

FIG. 3. Absolute value of the Fourier transform of Fig. 2 (full line). The peaks labeled 1 to 5 are due to the backscattering of the photoelectron from the first five shells. The dashed line shows the window function by means of which the contribution of the first shell has been separated from the other shells and from the noise.

filter function except for the side lobes at its flanks which are somewhat damped. Since the oscillations of the absorption coefficient below about 4 Å^{-1} contain contributions which are not due to EXAFS, we consider for further analysis only the part above 4 Å^{-1}. The filtered version of the EXAFS has now been fitted to Eq. (13) with $j=1$ for the first neighbors. Equation (13) also has to be multiplied by k^3 because the data set was multiplied by this factor. $\Phi_1(k)$ and $F_1(k)$ were taken from Ref. 17 and are shown in the Figs. 4 and 5 as dashed curves. The mean slope α_1 of $\Phi_1(k)$ is -0.63. For our Cu sample the jump height at the K edge is $J=3.52$. The energy resolution of the spectrometer is characterized by $\tau=5.3$ eV (Sec. II A). The coordination number N_1 and the loss factor D_1 in Eq. (13) can only be determined in the fit as product N_1D_1. Since in the present case N_1 is known to be 12 we can determine the loss factor D_1 for the first shell in Cu. We have used a standard nonlinear-least-squares fit to determine r_1, D_1, and σ_1. With $\Phi_1(k)$ and $F_1(k)$ from Ref. 17 we found for the first-neighbor distance in Cu $r_1=2.523$ Å. This value is too small by 0.025 Å compared to the known nearest-neighbor distance in Cu at 77 K, which is 2.548 Å.[27] The loss factor, $D_1^{\text{Cu}}=0.485$, means that about every second photoelectron does not contribute to the interference as a consequence of inelastic processes. The Debye-Waller displacement σ_1 was found to be 0.050 Å at 77 K.

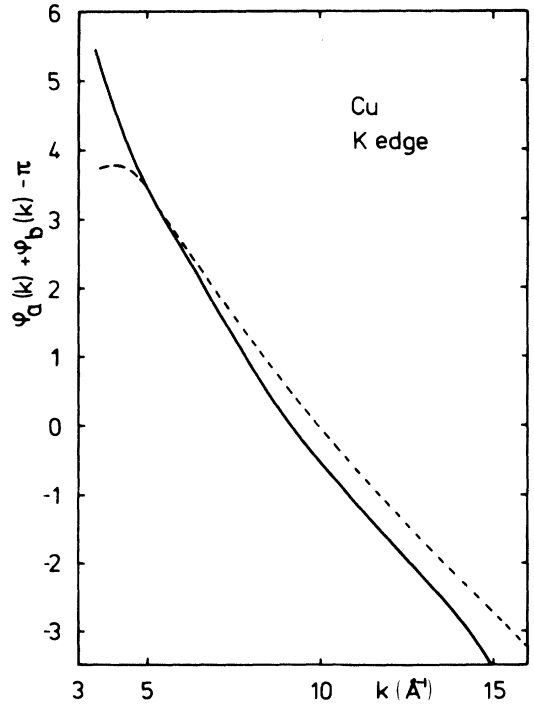

FIG. 4. Scattering phase shifts $\phi_1(k)=\phi_a(k)+\phi_b^1(k)-\pi$ for Cu–Cu in pure Cu according to Ref. 17 (dashed) and according to the present data set using a nearest-neighbor distance $r_1=2.548$ Å (full line).

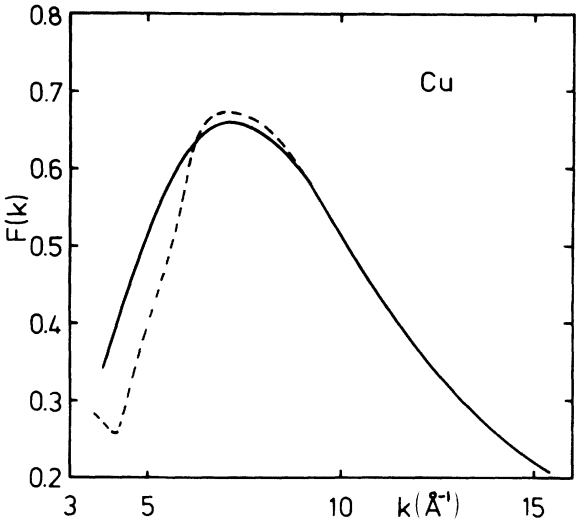

FIG. 5. Backscattering amplitude for Cu according to Ref. 17 (dashed) and from the present data set (full line).

Figure 6 shows a comparison of the experimental and fitted data for the first shell in Cu. It is obvious that the data are not fitted well below about 7 Å^{-1}. Apparently, the calculated phases and backscattering amplitudes are not optimal in that k range. We have therefore determined both quantities from the present data set. In a first step we have extracted the phase $2kr_1+\phi_a+\phi_b-\pi$ from the experimental data, and subtracted from it $2kr_1$, with the correct value

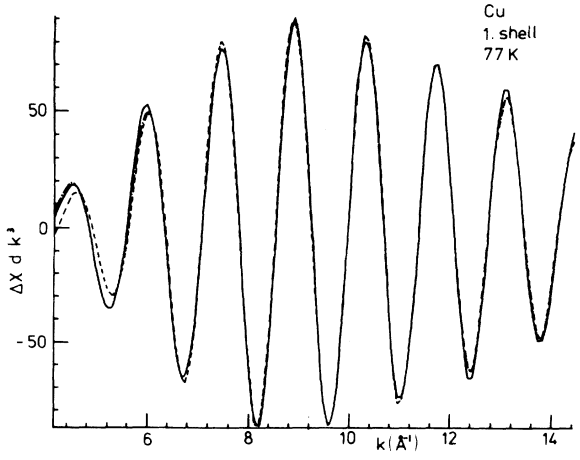

FIG. 6. Fit of the first-shell contribution in the EXAFS of Cu of Eq. (13) using the phase shifts and backscattering amplitudes of Ref. 17 (dashed curve) and those from Table II (dot-dashed curve).

$r_1 = 2.548$ Å. The resulting phase combination $\Phi = \phi_a + \phi_b - \pi$ is shown as solid curve in Fig. 4. With these scattering phases the fit improved by a factor of 1.7. Although now the zero crossing of the fitted curve agreed well with the experimental results, the amplitudes were still in poor agreement. Therefore we have also changed the backscattering amplitude as shown in Fig. 5 (full curve). Using both the improved phase shifts and amplitudes (Table II), we reached an overall improvement of the fit by a factor of 2.4 (Fig. 6). The result of the fit gave Cu–Cu

$$r_1 = (2.55 \pm 0.01)\ \text{Å}\ , \tag{14}$$

$$\sigma_1 = (0.05 \pm 0.01)\ \text{Å}\ , \tag{15}$$

$$D_1 = 0.495 \pm 0.05\ . \tag{16}$$

Note that the value σ for the mean relative displacement is not altered by the change in the scattering phases and amplitudes. The value $\sigma = (0.05 \pm 0.01)$ Å obtained in our fit agrees within the accuracy of the data with those obtained by Böhmer *et al.*[28] Using various lattice vibrational models these authors calculated values for σ between 0.052 and 0.060 Å. The value E_0 in Eq. (2) is not exactly defined since it depends on the chemical environment of the Cu atoms and on the zero of the potentials used to calculate $F(k)$ and $\Phi(k)$. Therefore we have allowed it to vary during the fit. According to Eq. (2) a change ΔE_0 in E_0 generates variations in k of

$$\Delta k = -m\Delta E_0/\hbar^2 k\ . \tag{17}$$

TABLE II. Backscattering amplitude $F(k)$ for Cu and scattering phase shifts $\phi_a + \phi_b - \pi$ for Cu as absorber (K edge) and as backscatterer deduced from the EXAFS in Fig. 2.

k (Å^{-1})	$F(k)$	$\phi_a + \phi_b - \pi$
4.0	0.365	4.67
4.5	0.430	4.00
5.0	0.510	3.43
5.5	0.575	2.97
6.0	0.620	2.57
6.5	0.645	2.16
7.0	0.660	1.72
7.5	0.655	1.28
8.0	0.645	0.85
8.5	0.625	0.48
9.0	0.600	0.13
10.0	0.515	−0.50
11.0	0.440	−1.11
12.0	0.365	−1.67
13.0	0.305	−2.22
14.0	0.260	−2.82
15.0	0.220	−3.55

Variations in E_0 are correlated with variations in r through the phase of the sin in Eq. (13). But as has been pointed out by Teo and Lee[17] errors in E_0 and r_1 fortunately do not compensate since ΔE is most effective at low values of k whereas Δr is most effective at high values of k. This reduces the correlation between r and E_0 and avoids false minima for r due to errors in E_0. We could corroborate this fact. Indeed, in repeating the data analysis with $E_0 = 8994$ eV rather than 9005 eV, we found in the fit the same values for r_1, σ_1, and D_1 but $\Delta E_0 = +10.0$ eV, giving the same value $E_0 + \Delta E_0$ and the same r in both approaches. The correlation between E_0 and r_1 turned out to be only 7%.

The errors quoted in Eqs. (14)–(16) have been determined in the following way. We have first kept r_1 fixed during a fit giving it values in the vicinity of 2.55 Å and leaving only σ_1, N_1D_1, and ΔE_0 free to vary. We then have plotted the error Ω (being the sum of the squares of the deviations between experiment and fit) versus r_1. This plot shows the steepness of the minimum along the direction r_1 in parameter space. The distance Δr away from 2.55 Å at which $\Omega = 2\Omega_{\min}$ is the error quoted in Eq. (14). Two points are worth to be noted in this regard. First, in the case of the first shell in pure Cu the correlation between r_1 on the one side and N_1D_1 and σ_1 on the other is very small (only +1%). This is one of the reasons why the distance of a shell with only one type of atom can be determined very accurately (better than 1%). On the contrary, N_1D_1 and σ_1 are correlated strongly (90%). In principal the different k dependence of both parameters should make it possible to separate the two. This requires a sufficiently long data set with a low-noise level. It is therefore very helpful, whenever possible, to measure the EXAFS at low temperatures in order to reduce the dynamical Debye-Waller damping. Due to the correlation we estimate the error in N_1D_1 to be about 10% and that of σ_1 to be about 10–15%. Second, when the first shell contains more than one type of atoms the errors can be appreciably larger. Great care is required if the contribution of one type is much larger than that of the other or if the two types of atoms have similar Z, i.e., similar backscattering power. In these cases there can also be a strong correlation between the distances and the amplitudes.

We have also analyzed the third shell in Cu. With the new phases and amplitudes from Table II the fit gave the following values for the parameters for Cu–Cu:

$$r_3 = (4.41 \pm 0.02)\ \text{Å}\ , \tag{18}$$

$$\sigma_3 = (0.06 \pm 0.01)\ \text{Å}\ , \tag{19}$$

$$D_3 = 0.23 \pm 0.04\ , \tag{20}$$

$$E_0 + \Delta E_0 = 8995\ \text{eV}\ . \tag{21}$$

There are 24 Cu atoms in the third shell at a distance of 4.414 Å.[27] About three-quarters of the photoelectrons are lost by inelastic processes. It is noteworthy that the phases and amplitudes of Teo and Lee[17] give a distance of 4.37 Å which is again 1% smaller than the correct value just as for the first shell. The quality of the fit is very similar to the one of the first shell. Finally we have analyzed the influence of the finite-energy resolution of the spectrometer on the parameter r, σ, and D. We have already seen in Sec. II A that the finite-energy resolution reduces most strongly the EXAFS oscillations at low k values. Thus, neglecting the finite energy is expected to result in too small values for σ and for D. This is what we have found by analyzing the data for the first shell of Cu with $\tau=0$ in Eq. (13). The distance is unchanged, whereas σ becomes smaller by 5% and D by 10%; i.e., the inelastic losses seem to be larger by 10% than they are in reality. The error is larger for the higher shells. For instance, for the third shell in Cu at $r=4.41$ Å σ becomes smaller by 15% and the loss factor by 30%. If τ is larger than in the present case ($\tau=5.3$ eV) the error will be higher correspondingly. If a shell contains more than one type of neighbors the problems arising from neglecting the finite value of τ are more serious due to correlations between the distances and the amplitudes of the different contributions.

B. Results for α-AlCu

The second model substance we have investigated is α-AlCu with 0.5 at.% Cu (Table I). It is known that a supersaturated solid solution (SSSS) of Cu in Al can decompose in different metastable and stable phases depending on the heat treatment given to the solution. The sequence of decomposition is[29]

$$\text{SSSS} \rightarrow \text{Guinier-Preston(GP)-zones} \rightarrow \theta'' \rightarrow \theta' \rightarrow \theta \ , \qquad (22)$$

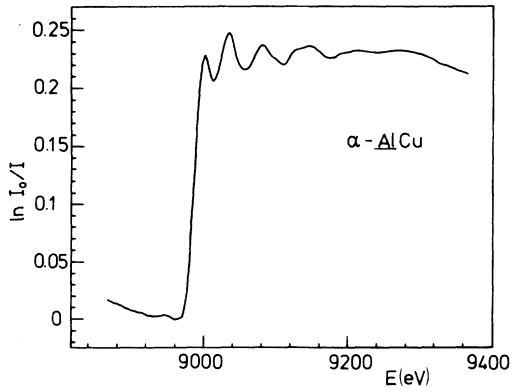

FIG. 7. EXAFS data for α-AlCu (0.5 at.% Cu) at 77 K. The edge jump $J=0.23$.

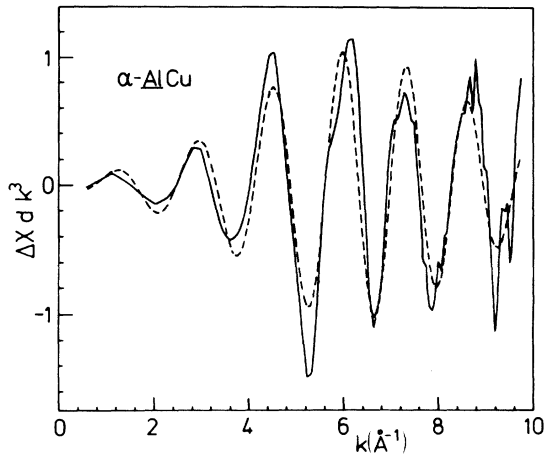

FIG. 8. EXAFS spectrum for α-AlCu from Fig. 7 after multiplication by k^3 and background subtraction. The contribution of the first shell is shown as dashed line.

if the solution contains 2 at.% Cu. On the other hand if the temperature does not exceed room temperature and if the concentration of Cu is low as 0.5 at.% none of these precipitations is obtained.[30–32] By a fast quench of a 0.5 at.% Cu alloy to 0 °C and by keeping the sample at room temperature (this is the treatment chosen here) the SSSS can be frozen in although it appears that some clustering of the Cu atoms occurs.[33] Figure 7 shows the EXAFS data for our 0.5 at.% AlCu alloys measured in transmission at 77 K. The analysis proceeds in an analogous way to that of pure Cu. The background subtracted EXAFS (full line in Fig. 8) is Fourier transformed (Fig. 9) and the contribution of the first shell has been extracted by means of the dashed-window function. The Fourier-backtransformed first-shell contribution

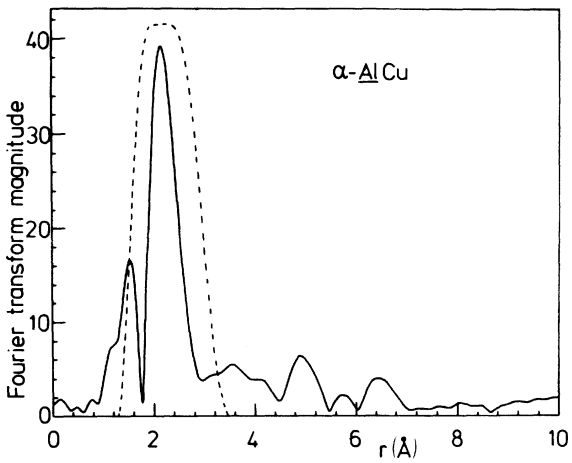

FIG. 9. Absolute value of the Fourier transform of Fig. 7 for α-AlCu (full line). The dashed line shows the window function used to extract the contribution of the first shell.

is shown as dashed line in Fig. 8. This first-shell contribution has been fitted to Eq. (13) (after multiplying that by k^3 as has been done with the raw data). First we have assumed in the fit that a Cu atom has 12 Al neighbors but no Cu neighbors; i.e., we have ignored possible clustering of Cu atoms. The backscattering amplitudes for Al and the scattering phase shifts $\phi_a + \phi_b - \pi$ for Cu–Al used were those calculated by Teo and Lee.[17] The fit, shown in Fig. 10, gave the following values for the parameters for Cu–Al:

$$r = (2.79 \pm 0.03)\ \text{Å}\ , \tag{23}$$

$$\sigma = (0.08 \pm 0.016)\ \text{Å}\ , \tag{24}$$

$$D = 0.32 \pm 0.04\ . \tag{25}$$

We have also fitted the data set assuming Al and Cu neighbors in the first shell. This fit did not change the Cu–Al parameters within the errors quoted and gave a small contribution of Cu–Cu backscattering

$$r = (2.48 \pm 0.03)\ \text{Å}\ , \tag{26}$$

$$\sigma = 0.06 \pm 0.015\ , \tag{27}$$

$$N = 0.4,\ D = 0.495\ , \tag{28}$$

Eq. (16), from the fit improved by about a factor of 2 when the first shell contains Al and Cu neighbors. The number of Cu atom adjacent to another Cu atom in an *Al*Cu alloy with 0.5 at.% of Cu distributed statistically is 0.06. The actually observed number of Cu neighbors is 0.4 which indicates that, indeed, some Cu–Cu clustering occurs in an 0.5 at.% alloy.[33]

An approximate value for the Cu–Al distance in a dilute *Al*Cu alloy can be calculated from the lattice parameter change observed when Cu is dissolved in Al. According to Pearson[27] it is $\Delta a = -0.358$ Å/100 at.% Cu. This corresponds to a volume change in a finite crystal of $(\Delta V/V)_f = -0.243$. The local volume change around a Cu atom is that which would be observed in an infinite crystal.[34] This can be calculated in a continuum approximation as $(\Delta V/V)_{\text{inf}} = (\Delta V/V)_f \gamma^{-1}$. The parameter γ depends on the elastic constants of the matrix and has the value 1.44 for Al.[35] Thus, we get

$$(\Delta V/V)_{\text{inf}} = -0.168 \tag{29}$$

in α-*Al*Cu. If this volume change were confined totally to the first-neighbor shell around a Cu atom, it would imply a Cu–Al distance of 2.69 Å compared to 2.79 Å found by EXAFS and compared to 2.85 for the first-neighbor Al–Al distance in metallic Al. The discrepancy between the lattice-parameter value and the EXAFS value is not astonishing. First, it is not obvious that the lattice distortion around a Cu atom is confined to the first shell. Second, the lattice parameter changes have been measured on samples containing up to 3 at.% Cu. It is known that in those samples, phase separation and precipitations [Eq. (23)] occur at room temperature which are accompanied by strong lattice-parameter changes.

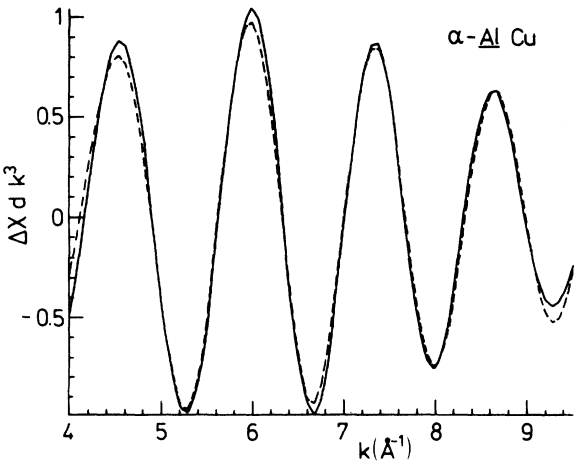

FIG. 10 Fit of the first shell in the EXAFS of α-*Al*Cu to Eq. (13) assuming 12 Al neighbors to a Cu atom. The dashed curve is the result of the fit.

C. Results for θ-$CuAl_2$

Figure 11 shows the EXAFS measured in transmission on the focused beam line at SSRL for the phase θ-$CuAl_2$. The phase is tetragonal (Fig. 12) and has lattice parameters $a = (6.063 \pm 0.003)$ Å and $c = (4.872 \pm 0.003)$ Å.[24] Each Cu atom has eight Al neighbors at 2.584 Å and two Cu neighbors at 2.436 Å. According to Havinga *et al.*[24] the composition $CuAl_2$ is slightly outside the range of the single phase region in the Al–Cu phase diagram and the stable compound has a little excess of Al. The phase boun-

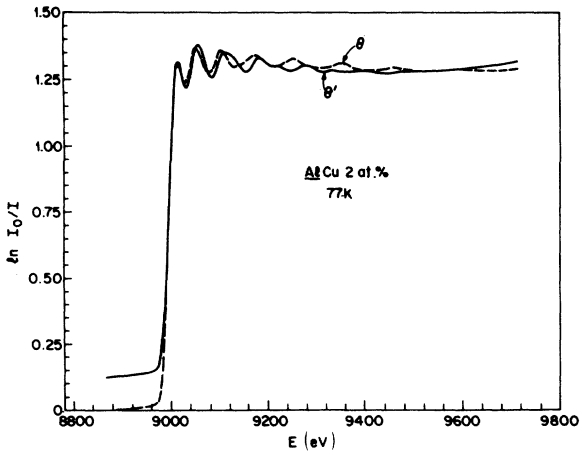

FIG. 11. EXAFS data for the phases θ' and θ in Al-Cu measured at 77 K on the focused beam line at SSRL.

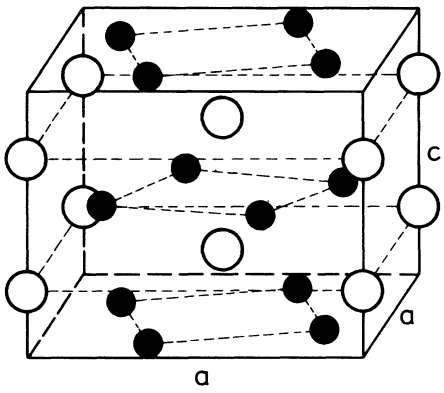

FIG. 12. Unit cell of the tetragonal Al-Cu phase θ. The open and full circles represent Cu and Al atoms, respectively.

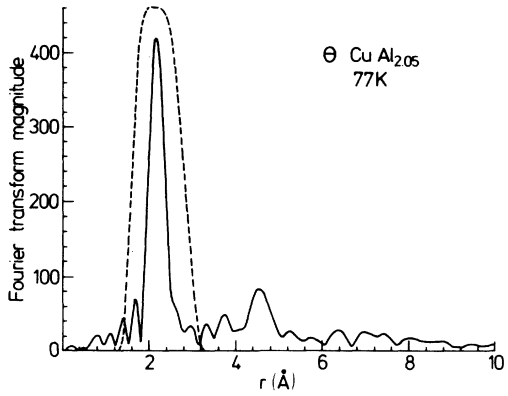

FIG. 14. Absolute value of the Fourier transforms of the EXAFS for θ.

dary is at $CuAl_{2.05}$. The phase θ can also be prepared from a supersaturated solid solution of Cu in Al. Then the compound forms above about 300 °C. We have prepared the θ phase in both ways and will first show the result of the analysis for θ $CuAl_{2.05}$ prepared by alloying the elements.

The data have been analyzed in the same way as described in Sec. IV B, except that now we have used the loss factors Eqs. (16) and (25) in order to determine the coordination numbrs for the first shell. Figure 13 shows the EXAFS $\Delta\chi dk^3$ after multiplication with k^3 and after background subtraction. Also shown are the contribution of the first shell. The corresponding Fourier transform is given in Fig. 14. For the fit of the filtered EXAFS of θ (dashed curve in Fig. 13) we have assumed Cu and Al neighbors in the first shell. The result of the fit is given in Table III and in Fig. 15. The distances are in excellent (error <1%) and the coordination numbers in reasonable (error 15–20%) agreement with those determined from x-ray diffraction. The substantially larger error in N is due to the strong correlation between N and σ (up to 90%).

A point of crucial importance in the fitting procedure adapted here is the number of shells in Eq. (13) on which the experimental data are fitted. In the present case we know that the first shell contains one type of Al and one type of Cu atoms. But it is interesting to see what the result of the fit is if we try to fit the data with only Al neighbors in the first shell. The result is given in Table III. The Cu–Al distance is again in very good agreement with the known value. Although N_{Al} seems to be reasonable the value of σ is almost zero which is too small. If we constrain σ to be 0.065 than we obtain $N_{Al}=12.3$ which is higher by 50% than the value it should be. The quality of the fit deteriorates by a factor of 12. Therefore, in the present case it is pretty obvious which fit is more significant. But the analysis is not always so unambiguous as in this case. We will come

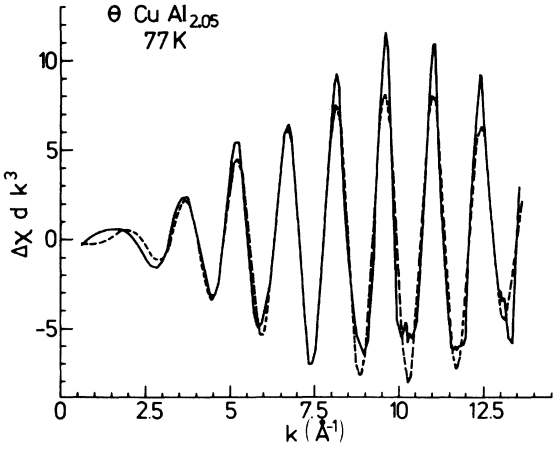

FIG. 13. EXAFS spectrum for θ after multiplication by k^3 and background subtraction. The contribution of the first Al and Cu shells is given as dashed line.

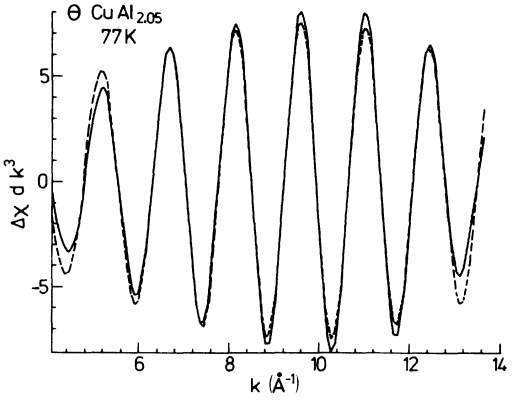

FIG. 15. Fit of the first shell in the EXAFS of θ to $\Delta\chi dk^3$ [Eq. (13)]. It has been assumed that a Cu atom has first Cu and Al neighbors.

TABLE III. Fit of the EXAFS of the first Cu and Al shells in θ to $\Delta\chi dk^3$ [Eq. (13)]. In order to show the reliability of the fitting procedure it has been assumed that the shell contains only Al and Cu neighbors at a wrong distance. The fit then deteriorates by a factor of 12.

	EXAFS	Only Al		θ-$CuAl_{2.05}$ wrong r_{Cu}	θ precipitation in 2 at.% *Al*Cu	Bragg[a]
Cu–Al						
r (Å)	2.57 ± 0.02	2.58	2.58	2.58	2.56 ± 0.02	2.583
σ (Å)	0.065 ± 0.013	0.002	0.065	0.000	0.060 ± 0.012	
N	7.6 ± 1.0	7.3	12.3	7.3	7.7 ± 1.0	8
Cu–Cu						
r (Å)	2.44 ± 0.02			2.85	2.44 ± 0.02	2.436
σ (Å)	0.065 ± 0.013			0.47	0.063 ± 0.012	
N	2.3 ± 0.4	0	0	0.1	2.3 ± 0.4	2

back to this point in Sec. II D.

We have also checked the influence of a wrong assumption in a distance (the Cu–Cu distance) on the fit. Keeping the Cu–Cu distance fixed at a value (2.85 Å) which is too large by 0.4 Å the fit reduces the whole contribution of the Cu neighbors to zero by making σ very large and N_{Cu} very small (Table III). The fit is practically identical with that one where N_{Cu} was set zero. This result is not surprising in view of the great accuracy achieved in the determination of interatomic distances. Finally, we show in Table III the result of the analysis of the θ phase obtained by precipitation at 400 °C in a 2 at.% *Al*Cu alloy. Within the accuracy of the data the result is identical with that obtained on the intermetallic compound. This implies that by the heat treatment given to the 2 at.% *Al*Cu alloy (Table I) all the Cu precipitates into the θ phase and the amount of Cu left in solution must be very small.

D. Results for the θ' phase

The phase θ' in the system Al-Cu is a metastable phase of tetragonal symmetry with lattice parameters $a = 4.04$ Å and $c = 5.8$ Å.[25] A Cu atom has eight Al neighbors at 2.49 Å, four Cu neighbors at 4.04 Å, and eight more Cu neighbors at 4.08 Å (Fig. 16). θ' forms from a supersaturated solution (2 at.% Cu) only above 150 °C. Above 300 °C it transforms into

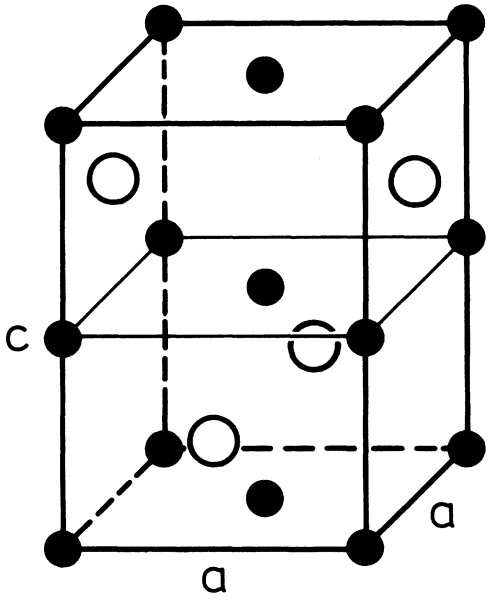

FIG. 16. Unit cell of the tetragonal Al-Cu phase θ'. The open and full circles represent Cu and Al atoms, respectively.

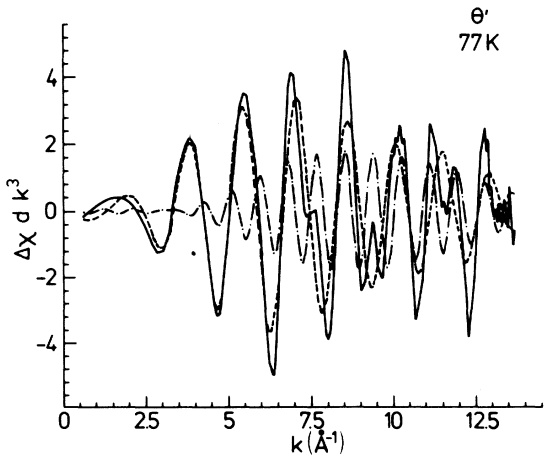

FIG. 17. EXAFS spectrum for θ' after multiplication by k^3 and background subtraction. The contribution of the first Al and Cu shells are given as dashed and dot-dashed curves.

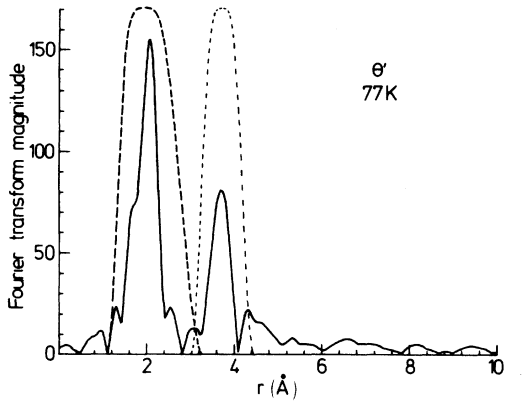

FIG. 18. Absolute value of the Fourier transform of the EXAFS for θ'. The contribution of the first Al and Cu shells are well separated.

θ. The average composition of θ' is again $CuAl_2$. Figure 11 shows the EXAFS measured on θ'. The difference in the atomic arrangements in θ and θ' is reflected in the different EXAFS spectra. The analysis follows again the scheme outlined above. The inelastic loss factors D_{Cu} and D_{Al} were taken from Eqs. (20) and (25). Figure 17 shows the EXAFS $\Delta\chi dk^3$ for θ' and the contribution of the first Al and Cu shells which are well separated from one another as shown in the Fourier spectrum (Fig. 18). The fit of the first Al shell is given in Fig. 19 and Table IV. The distance agrees very well with that known from x-ray diffraction. The coordination number is too high by 20%. We have also tried a fit in which it was assumed that the first shell contains Al and Cu. The result of this fit is also given in Table IV. Within the accuracy of the analysis the fit

TABLE IV. Fit of the EXAFS of the first Al and Cu shells in θ' to the expression $\Delta\chi dk^3$. The shell centered at 2.5 Å is known to contain only Al. If the fit is made with Al and Cu neighbors, N_{Cu} turns out to be almost zero.

θ'	EXAFS first Al shell		First Cu shell	Bragg[a]	
Cu–Al					
r (Å)	2.48 ± 0.02	2.47		2.487	
σ (Å)	0.064 ± 0.012	0.057			
N	9.6 ± 1.5	9.7		8	
Cu–Cu					
r (Å)		2.40	4.07 ± 0.04	4.071	4.040
σ (Å)		0.041	0.066 ± 0.015		
N		0.3	11.0 ± 1.5	8	4

[a]Reference 25.

gives $N_{Cu} \approx 0$. The quality of this fit is only improved by 19% compared to that one with only Al neighbors. We conclude that in our θ' phase there are no Cu–Cu neighbors in the shell around 2.50 Å. The first Cu–Cu neighbors are at 4.07 Å as shown in Table IV and Fig. 20. There are two types of Cu neighbors one at 4.04 Å and one at 4.08 Å. In the fit we cannot distinguish between these two. The fit with one Cu shell gives a distance which is in very good agreement with the average Cu distance of 4.061 Å. Also the coordination number is only 9% smaller than the one determined from x-ray diffraction.

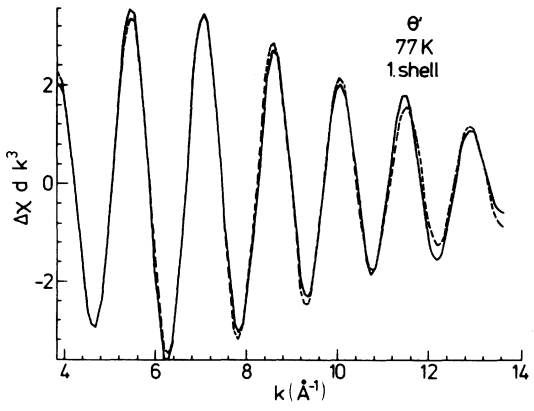

FIG. 19. Fit of the first Al shell in the EXAFS of θ' to $\Delta\chi dk^3$.

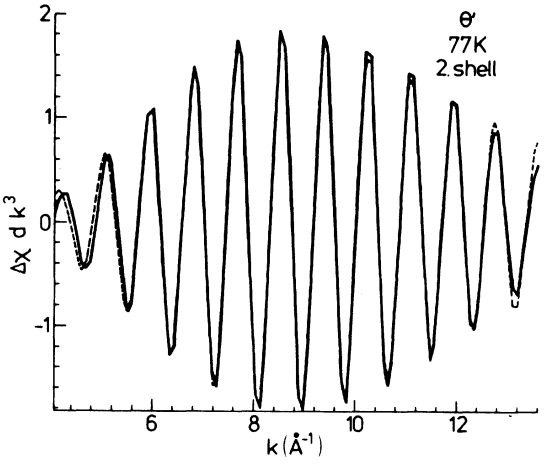

FIG. 20. Fit of the first Cu shell in the EXAFS of θ to $\Delta\chi dk^3$.

V. CONCLUSION

The present approach of data analysis of EXAFS spectra has turned out to give satisfactory results. In fact, the interatomic distances for the first-neighbor shells can be determined with an accuracy of 1%. The coordination numbers are less accurate due to their correlation with the Debye-Waller factor. Since there are only a few alternative ways for determining coordination numbers an accuracy of about 15% is quite reasonable. We estimate the error in the mean relative displacement σ to be about 20%. For pure Cu the value of σ obtained in a recent calculation agrees well with the presently determined value.

From Eqs. (16), (20), and (25) it can be seen that the inelastic photoelectron losses are substantial. Thus, their adequate determination is essential for the determination of coordination numbers. The present concept which is based on a comparison with model compounds of known structure requires an additional measurement but has been shown to be a practicable way. If we express the loss factors for our four systems in terms of a k-independent mean free path with $\tilde{D}=1$ we obtain the following values for λ(Cu–Cu): (7.3 ± 1.1) Å and (6.0 ± 0.7) Å for the first and third shell in pure Cu, (5.8 ± 1.0) Å in θ, and (5.9 ± 0.5) Å in θ'. The corresponding values for λ(Cu–Al) are (4.9 ± 0.6) Å in α, (4.8 ± 0.8) in θ, and (3.8 ± 0.4) in θ'. At the present time it is not possible to decide if the spread in our λ values is real or not. The values of λ quoted by Brundle[22] for photoelectron energies between 50 and 1000 eV range from 4 to 10 Å. This is the same magnitude as those obtained here. Hence we cannot give an estimation of the size of the r-independent loss factor $\tilde{D}$. With the present accuracy of the loss factors the description chosen here and that using a simple man free path are equivalent. Better theoretical values for λ and a higher accuracy in the determination of D_j are necessary in order to decide if the mean free path concept has to be extended as proposed in Eq. (12).

We have taken into account for the first time the effect of the finite energy resolution of the spectrometer. Neglecting this effect can easily produce errors of 10% for the nearest-neighbor shell and it increases with the interatomic distance. We have shown in Eq. (13) that the extension of the theory which takes this effect into account is very simple and it should make no problem to bypass this source of systematic errors in the data analysis.

Although the concept to separate the EXAFS contributions from different shells by Fourier transformation worked satisfactory in the present systems we have analyzed other systems where serious problems can occur. In fact, if a peak in a Fourier spectrum contains more than two contributions it is difficult to separate them. Three contributions can be untangled only if the contributing backscatters have substantially different backscattering power. We were able to analyze the first peak in the Fourier spectrum of θ (Fig. 14) because the backscattering powers of the Cu and Al are sufficiently different from one another. On the other hand in a *Cu*Fe alloy with 3 at.% of Fe, Cu shells ($Z=29$), and Fe shells ($Z=26$) with similar distances could not be separated from one another.

ACKNOWLEDGMENTS

The authors would like to thank Dr. B. M. Kincaid for many stimulating discussions. One of us (B.L.) would like to thank the Bell Laboratories for the great hospitality during his stay in the U.S. The experiments were performed at SSRL, which is partially supported by NSF Grant No. DMR 73-07692 in cooperation with the Stanford Linear Accelerator and U.S.-ERDA. The authors are indebted to the members of SSRL for the great help during the measurements.

---

*On leave of absence from Institut für Festkörperforschung, KFA Jülich, 5170 Jülich, Germany.

[1]D. E. Sayers, E. A. Stern, and F. W. Lytle, Phys. Rev. Lett. 27, 1204 (1971).
[2]E. A. Stern, Phys. Rev. B 10, 3027 (1974).
[3]B. M. Kincaid and P. Eisenberger, Phys. Rev. Lett. 34, 1361 (1975).
[4]F. W. Lytle, D. E. Sayers, and E. A. Stern, Phys. Rev. B 11, 4825 (1975).
[5]E. A. Stern, D. E. Sayers, and F. W. Lytle, Phys. Rev. B 11, 4836 (1975).
[6]B. M. Kincaid, thesis (Stanford University, 1974) (unpublished), and SSRP Report No. 75/03 (1975) (unpublished).
[7]P. H. Citrin, P. Eisenberger, and B. M. Kincaid, Phys. Rev. Lett. 36, 1346 (1976).
[8]S. P. Cramer, T. K. Eccles, F. Kutzler, K. O. Hodgsen, and S. Doniach, J. Am. Chem. Soc. 98, 8059 (1976).
[9]J. Jaklevic, J. A. Kirby, M. P. Klein, A. S. Robertson, G. S. Brown, and P. Eisenberger, Solid State Commun. 23, 679 (1977).
[10]G. S. Brown, P. Eisenberger, and P. Schmidt, Solid State Commun. 24, 201 (1977).
[11]G. Martens, P. Rabe, N. Schwentner, and A. Werner, Phys. Rev. Lett. 39, 1411 (1977).
[12]S. H. Hunter, A. I. Bienenstock, and T. M. Hayes, in *Structure of Non-Crystalline Materials*, edited by P. H. Gaskell (Taylor and Francis, London, 1977), p. 73.
[13]P. Eisenberger and B. M. Kincaid, Science 200, 1441 (1978).
[14]T. M. Hayes, J. Non-Cryst. Solids 31, 57 (1978).
[15]G. S. Knapp and F. Y. Fradin, in *Electron and Positron Spectroscopies in Materials Science and Engineering*, edited by O. Buck (Academic, New York, 1978).

[16]P. Eisenberger and G. S. Brown, Solid State Commun. 29, 481 (1971).
[17]B. K. Teo and P. A. Lee, J. Am. Chem. Soc. 101, 2815 (1979).
[18]C. A. Ashley and S. Doniach, Phys. Rev. B 11, 1279 (1975).
[19]P. A. Lee and G. Beni, Phys. Rev. B 15, 2862 (1977).
[20]S. H. Hunter, PhD. thesis (Stanford University) (unpublished) and SSRL Report No. 77/04 (unpublished).
[21]W. Heitler, *The Quantum Theory of Radiation* (Oxford University Press, New York, 1944), p. 204.
[22]C. F. Brundle, Surf. Sci. 48, 99 (1975).
[23]H. Hansen and K. Anderko, *Constitution of Binary Alloys* (McGraw-Hill, New York, 1958).
[24]E. E. Havinga, H. Damsma, and P. Hokkeling, J. Less Common Met. 27, 169 (1972).
[25]J. M. Silcock, T. J. Heal, and H. K. Hardy, J. Inst. Met. 82, 239 (1953-54).
[26]B. Lengeler, Philos. Mag. 34, 259 (1976).
[27]W. B. Pearson, *Handbook of Lattice Spacings and Structures of Metals and Alloys* (Pergamon, New York, 1958), Vol. 1.
[28]W. Böhmer and P. Rabe, J. Phys. C 12, 2465 (1979).
[29]A. Kelly and R. B. Nicholson, Prog. Mater. Sci. 10, 151 (1963).
[30]H. K. Hardy, J. Inst. Met. 79, 321 (1951); and 82, 236 (1953-54).
[31]J. P. Miraille, M. Levoy, C. Brichet, and B. Lacombe, Scr. Metall. 5, 1061 (1971).
[32]L. F. Mondolfo, *Aluminum Alloys: Structure and Properties* (Butterworths, London, 1976), p. 253.
[33]D. Turnbull, H. S. Rosenbaum, and H. N. Treaftis, Acta Metall. 8, 277 (1960).
[34]J. D. Eshelby, J. Appl. Phys. 25, 255 (1954).
[35]P. H. Dederichs and J. Pollmann, Z. Phys. 255, 315(1972).